Transport pathways of carbon monoxide from Indonesian fire pollution to a subtropical high-altitude mountain site in western North Pacific

Saginela Ravindra Babu[1*], Chang-Feng Ou-Yang[1], Stephen M. Griffith[1], Shantanu Kumar Pani[1], Steven Soon-Kai Kong[1], and Neng-Huei Lin[1,2*]

[1]Department of Atmospheric Sciences, National Central University, Taoyuan 32001, Taiwan.

[2]Center for Environmental Monitoring and Technology, National Central University, Taoyuan 32001, Taiwan.

Correspondence to**:** S. Ravindra Babu (baburavindra595@gmail.com) and Neng-Huei Lin (nhlin@cc.ncu.edu.tw).

Abstract: Dry conditions associated with El Niño and a positive Indian Ocean Dipole (IOD) are known to have caused major fire pollution events and intense carbon emissions over a vast spatial expanse of Indonesia in October 2006 and 2015. During these two events, a substantial increase in carbon monoxide (CO) mixing ratio was detected by in-situ measurements at Lulin Atmospheric Background Station (LABS, 23.47°N 120.87°E, 2,862 m ASL) in Taiwan, the only background station in the subtropical western North Pacific region. Compared to the long-term October mean (2006-2021), CO was elevated by ~47.2 ppb (37.2%) and ~36.7 ppb (28.9%) in October 2006 and 2015, respectively. This study delineates plausible pathways for CO transport from Indonesia to LABS using MOPITT CO observations and MERRA-2 reanalysis products (winds and geopotential height (GpH)). Two simultaneously occurring transport pathways were identified: (i) horizontal transport in the free troposphere and (ii) vertical transport through the Hadley circulation (HC). The GpH analysis of both events revealed the presence of a high-pressure anticyclone over the northern part of the South China Sea (SCS), which played an important role in the free tropospheric horizontal transport of CO. In this scenario, CO in the free troposphere is transported on the western edge of the high-pressure system and then driven by subtropical westerlies to LABS. Simultaneously, uplifted CO over Indonesia can enter the HC and transfer to subtropical locations such as LABS. The vertical cross-section of MOPITT CO and MERRA-2 vertical pressure velocity supported the transport of CO through the HC. Further, the results revealed a distinct HC strength in two events (higher in 2006 compared to 2015) due to the

different El Niño conditions. Overall, the present findings can provide some insights into understanding the regional transport of pollution over Southeast Asia and the role of climate conditions on transport pathways.

Keywords: Indonesian fire pollution; Carbon monoxide; Lulin Atmospheric Background Station; Hadley circulation

1. Introduction

Fire activity over Southeast Asia (SEA), particularly over the Maritime Continent (MC, including Indonesia), is a severe environmental problem that causes widespread regional pollution in the lower troposphere and impacts atmospheric chemistry, air quality, and climate at regional to global scales. Over the MC, fires occur predominately in the dry season (August to October) and particularly during the periods of drought, often associated with the positive phase of El Niño-Southern Oscillation (ENSO) events (Duncan et al., 2003a; van der Werf et al.,2008, 2017; Field et al., 2009, 2016). A recent study has also highlighted the role of the Indian Ocean Dipole on MC fire activity (Pan et al., 2018). For example, dry conditions associated with the positive IOD during the ~~the extreme~~ 2015/16 El Niño and ~~weak~~ 2006/07 El Niño events led to increased fire activity over Indonesia and the wider MC (van der Werf et al.,2008; Chandra et al., 2009; Nassar et al., 2009; Huijnen et al., 2016; Field et al., 2016). Due to these intense fires, an enormous amount of carbon emissions was released into the atmosphere in the form of carbon dioxide (CO_2), carbon monoxide (CO), and methane (CH_4) (Huijnen et al., 2016; Field et al., 2016; Parker et al., 2016; Heymann et al., 2017). The impact of these two Indonesian fire events on carbon emissions, tropospheric trace gases, aerosol composition, and air quality has been extensively discussed in the literature ~~These two Indonesian fire events and the associated impacts on carbon emissions, trace gas and aerosol composition, and air quality has been extensively discussed in the literature~~ (Chandra et al., 2006; Logan et al., 2008; Chandra et al., 2009; Nassar et al., 2009; Huijnen et al., 2016; Field et al., 2016; Heymann et al., 2017; Ravindra Babu et al., 2019). For example, the fire carbon emissions during September-October 2015 over Maritime SEA were the largest since 1997 (Huijnen et al., 2016). By using Greenhouse gases Observing SATellite (GOSAT) data, Parker et al. (2016) reported the strong enhancement of CO_2 and CH_4 over the Indonesian region.

CO is a significant emission from the combustion of fossil fuels and biomass (forest and savanna fires, biofuel use, and waste burning) and is widely used as a tropospheric tracer for these sources (Ou-Yang et al., 2014; Pani et al., 2019). Inter-annual variability of CO in the tropics and sub-tropics is largely linked to year-by-year changes in biomass burning (BB) emissions. Indonesian fires often emit large quantities of CO by incomplete combustion associated with the occurrence of peat fire pollution. Although CO is not a direct greenhouse gas (GHG), it does have a global warming potential due to its chemical reactions in the atmosphere. CO is also an ozone (O_3) precursor in the troposphere, and indirectly increases radiative forcing (0.23 +/- 0.05 W m_{-2}) through the production of O_3 and CO_2 and depletion of hydroxyl radical, the primary chemical reactant with CH_4 in the atmosphere (IPCC, 2013). ~~For instance, CO oxidation produces CO_2 and indirectly ozone (O_3), both of which are GHGs, and depletes hydroxyl radical (OH) concentrations, thus extending the lifetime of CH_4, another GHG in the atmosphere (IPCC, 2013).~~ The lifetime of CO in the free troposphere is ~ two months, thus can be a tracer from polluted upwind regions to remote downwind areas (Cooper et al., 2012). Some of the studies reported the influence of Indonesian fire activity and the transport of CO from Indonesia to the Indian Ocean, Southern Pacific, and western Pacific Ocean (Matsueda and Inoue, 1999; Pochanart and Akimoto, 2003; Nara et al., 2011; Matsueda et al., 2002, 2019). However, the underlying transport mechanisms sending this fire pollution to downwind northern hemisphere subtropical locations, particularly transport to high-altitude background locations in the western north Pacific are still unclear.

~~As shown in **Figure 1**, the Lulin Atmospheric Background Station (LABS, 23.47°N 120.87°E, 2862 m ASL) located in central Taiwan was constructed in 2006 and~~ Taiwan is located downwind of East Asia and Southeast Asia, which are major air pollutant source regions. As result, Lulin Atmospheric Background Station (LABS, 23.47°N 120.87°E, 2862 m above sea level), was constructed in 2006 to study the transboundary transport of these air pollutants and their impact on Taiwan. ~~is the only high-altitude background station in the western Pacific region for monitoring the long-term variability of atmospheric compositions and also studying the influence of continental outflow and long-range transported pollution (Lin et al., 2013; Ou-Yang et al., 2014, 2022; Ravindra Babu et al., 2022). The~~ LABS is not affected by local sources, i.e., industrial and traffic emissions ~~often found within the free troposphere~~, making it an ideal site for measuring long-range transport of air pollutants, complementing the global network of the Global Atmospheric Watch (GAW) in the East Asia region where no other high-altitude background

Formatted: Subscript
Formatted: Superscript
Formatted: Subscript
Formatted: Subscript
Formatted: Subscript

station is available (Ou-Yang et al., 2014, 2022). In the framework of Seven South-East Asian Studies (7-SEAS, Reid, et al., 2013; Lin et al., 2013; Wang et al., 2015), several studies at LABS have reported on the long-range transport of northern peninsular Southeast Asia (PSEA) BB pollutants to Taiwan through the low-level jet (LLJ) and the related impacts on air quality and chemistry over Taiwan (Ou-Yang et al., 2012, 2014; Lin et al., 2013; Chuang et al., 2016; Chi et al., 2016; Tsay et al., 2016; Hsiao et al., 2016; Lin et al., 2017; Park et al., 2019; Pani et al., 2016, 2019; Huang et al., 2019; Huang et al., 2020; Ravindra Babu et al., 2022). However, to date, no studies have shown the potential influence of Indonesian fire activities on LABS measurements and the BB pollution from Indonesian fires reaching LABS. Surprisingly, the extensive fire events in 2006 and 2015 allowed us to track CO concentrations from the Indonesian peat fires to LABS in Taiwan. By combining in-situ and satellite CO measurements and large-scale circulation parameters from reanalysis products, we identified plausible transport pathways from Indonesia to LABS.

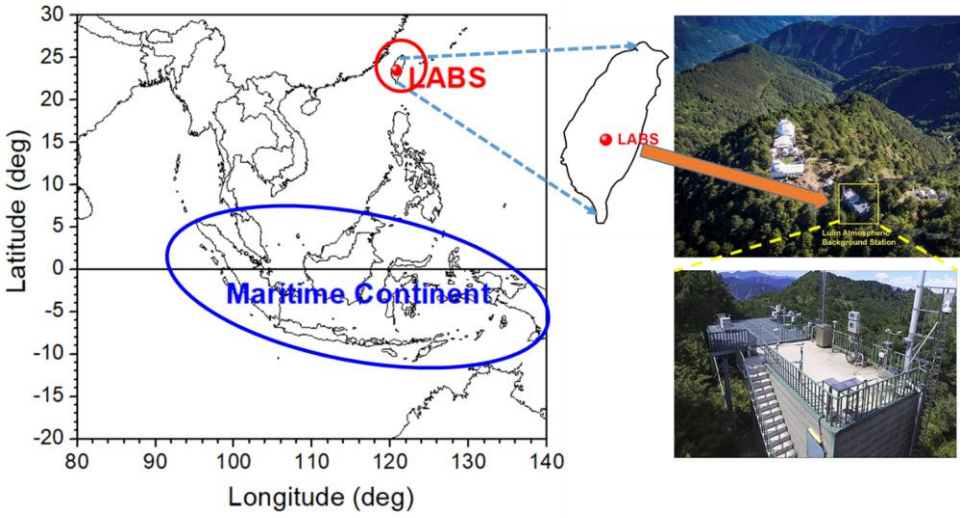

Figure 1. Geographic location of the Maritime Continent and Lulin Atmospheric Background Station (LABS, 23.47°N 120.87°E, 2862 m ASL), Taiwan.

2. Site description, ~~Data~~ data and methodology

2.1 Site description

LABS is located on the summit of Mount Lulin and is shown in Figure 1, along with the location of the Maritime Continent. Hiking is the only way to access LABS, taking about 30 minutes from the nearest parking lot. There are no known point emission sources at the summit or in the surrounding area with the exception of the occasional maintenance activity at the Lulin Observatory. Because of the high altitude of LABS, measurements there are not affected by local pollution from factories, traffic, and other domestic sources; rather, it is strategically located to monitor long-range transported air pollutants from the Asian continent. More details about the instruments and their specifications can be found in Sheu et al., 2009.

2.2 In-situ measurements

Details of the CO and various meteorological measurements at LABS employed in the current study have been previously described in detail (Sheu et al., 2009; Ou-Yang et al., 2014; Ravindra Babu et al., 2022) and are thus only briefly described here. The long-term monthly mean of various meteorological parameters such as temperature, relative humidity, wind speed, and wind direction along with CO at LABS can be found in **Sup. Figure 1**. The overall mean temperature (relative humidity) was about 10.5^{o}C (~80%), with monthly mean temperatures ranging between ~5 and 14^{o}C. Local wind direction is mostly from the southwest and to a lesser extent from the northeast. Long-term monthly mean in CO shows distinct seasonal patterns with a springtime maximum and a summertime minimum at LABS. CO ~~mixing ratios~~measurements were measured by a nondispersive infrared (NDIR) analyzer (APMA-360, Horiba, Japan) at LABS. Hourly averages of the 6-s data were analyzed in this study. The detection limit of the NDIR is ~20 ppb (1σ) (Zellweger et al., 2009); more details about CO measured at LABS can be found in Ou-Yang et. (2014). The magnitude of the CO concentration enhancement in 2006 and 2015 above the long-term background was determined by comparing a 16-year average (2006-2021) of October CO data at LABS. We obtained the percentage change in CO relative to the respective background using Equation 1:

$$\text{Relative change in percentage} = \left(\frac{x_i - \bar{x}}{\bar{x}}\right) \times 100 \qquad \text{(Eq. 1)}$$

where x_i represents the monthly mean of October in 2006 and 2015, and $\bar{x}$ is the corresponding monthly long-term mean calculated using the data from 2006 to 2021 (Ou-Yang et al., 2014).

2.~~2~~ 3 Satellite measurements

Formatted: Font: Bold

CO observations from the Measurement of Pollution in the Troposphere (MOPITT, version 8) instrument were also utilized in this study (Worden et al., 2010; Deeter et al., 2019). MOPITT is a multi-channel Thermal InfraRed (TIR) and Near InfraRed (NIR) instrument operating onboard the sun-synchronous polar-orbiting NASA Terra satellite. V8 CO products, consisting of a CO profile at ten pressure levels, have been validated; more details about the retrieval algorithm, validation, and ~~the~~ uncertainties of MOPITT CO can be found in Deeter et al. (2019). In addition to the MOPITT measurements, we utilized CO from the Atmospheric Infrared Sounder (AIRS) on the NASA Aqua satellite, which provides CO at different vertical levels twice daily and near-global coverage. AIRS uses wavenumbers 2,183-2,200 cm^{-1} (4.58-4.5 μm) for retrieving CO (McMillan et al., 2005). Version 8, level 3 CO product, available at 1° ×1° resolution at various pressure levels, was utilized in the present study. AIRS data were downloaded from the following website https://disc.gsfc.nasa.gov/datasets/AIRS3STM_7.0 (AIRS project., 2019). AIRS sensitivity to CO is broad and optimal in the mid-troposphere between approximately 300 and 600 hPa (Warner et al., 2007; Warner et al., 2013; AIRS project., 2019). CO retrievals have a bias of 6-10% between 900 hPa and 300 hPa with a root mean square error of 8-12 % (McMillan et al., 2011).

Apart from MOPITT and AIRS CO data, we used Moderate Resolution Imaging Spectroradiometer (MODIS) collection 6.1 daily active fire hot spot data from 2006~~ 2020~~ 2021 over Indonesia (Giglio et al., 2016).

2.3 MERRA-2 Reanalysis products

We also utilized monthly mean geopotential height (GPH), wind vectors (zonal and meridional wind speed), and pressure vertical velocity from the Modern-Era Retrospective Analysis for Research and Applications, version 2 (MERRA-2). ~~Modern-Era Retrospective Analysis for Research and Applications, version 2 (MERRA-2) monthly mean geopotential height (GpH) wind vectors (zonal and meridional) and vertical pressure velocity (omega) during the study period were utilized.~~ MERRA-2 is the latest atmospheric reanalysis data produced by the NASA Global Modeling and Assimilation Office (GMAO) (Gelaro et al., 2017). The horizontal resolution of MERRA-2 reanalysis is $0.5^{o} \times 0.625^{o}$. MERRA-2 data are available online through the NASA Goddard Earth Sciences Data Information Services Center (GES DISC; https://disc.gsfc.nasa.gov/, last access: 11 September 2022).

3. Results and Discussion

3.1 Higher CO mixing ratios in October 2006 and 2015 over Maritime Continent and at LABS

Figure 2 shows the height-time cross-section of monthly mean CO over the Maritime Continent (MC) obtained from MOPITT and AIRS from 2003 to 2021. There is a significant inter-annual variability in the CO time series in **Figure 2** as observed by both instruments. The maximum CO mixing ratio for this time period was observed in the fall of 2006 and 2015; both were tied to El Niño events (Field et al., 2016; Ravindra Babu et al., 2019). Several studies have reported on the impact of the intense fire activity in 2006 and 2015 and on the release of significant carbon emissions and poor air quality over the wider Equatorial Asia region (Logan et al., 2008; Chandra et al., 2009; Field et al., 2016; Huijnen et al., 2016; Ravindra Babu et al., 2019). Even though 2009 and 2014 were El Niño years, the CO over MC was not as high as observed in 2006 and 2015. The weaker and shorter duration of fire activities could largely explain the lower CO over the MC in 2009 and 2014 in contrast to those in 2006 and 2015. Furthermore, **Figure 3** shows the temporal variability of monthly mean CO from MOPITT and AIRS from January through December in both years 2006 and 2015, respectively. Both instruments show maximum CO enhancement in October compared to the remaining months in 2006 and 2015. Overall, it is clear from **Figures 2** and **3** that in October 2006 and 2015, CO over the Maritime Continent in the entire troposphere increased dramatically due to increased CO emissions near the surface from extreme fire activity (**Fig. 4c**).

Formatted: Font: Not Bold
Formatted: Line spacing: 1.5 lines
Formatted: Font: Not Bold
Formatted: Font: Not Bold
Formatted: Font: Not Bold
Formatted: Font: Not Bold
Formatted: Font: Not Bold

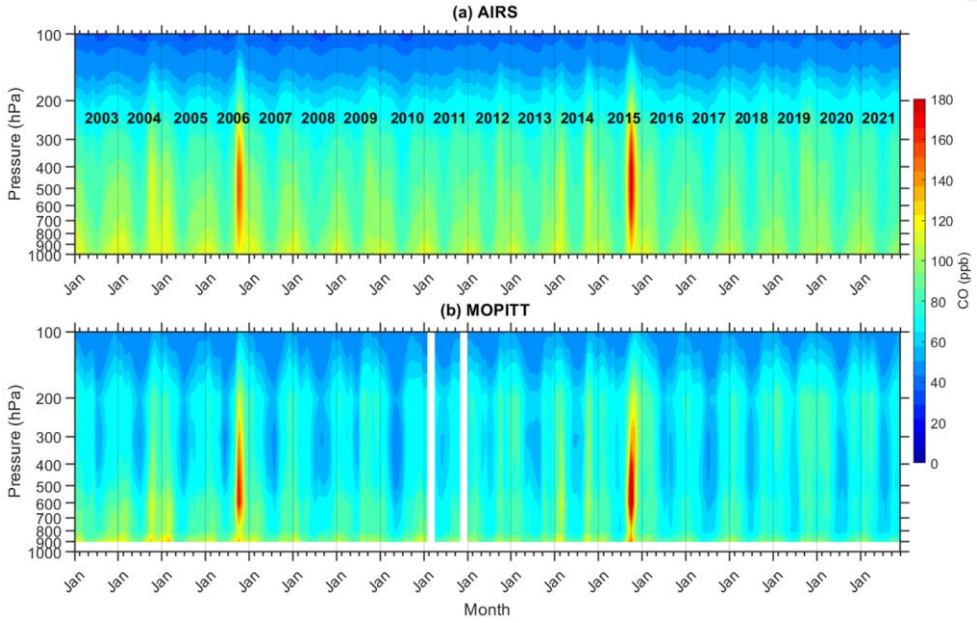

Figure 2. Pressure-time cross-section of monthly mean carbon monoxide observed over the Maritime continent (average over 90E-140E,10S-10N) during 2003-2021 obtained from (a) AIRS, and (b) MOPITT satellite measurements.

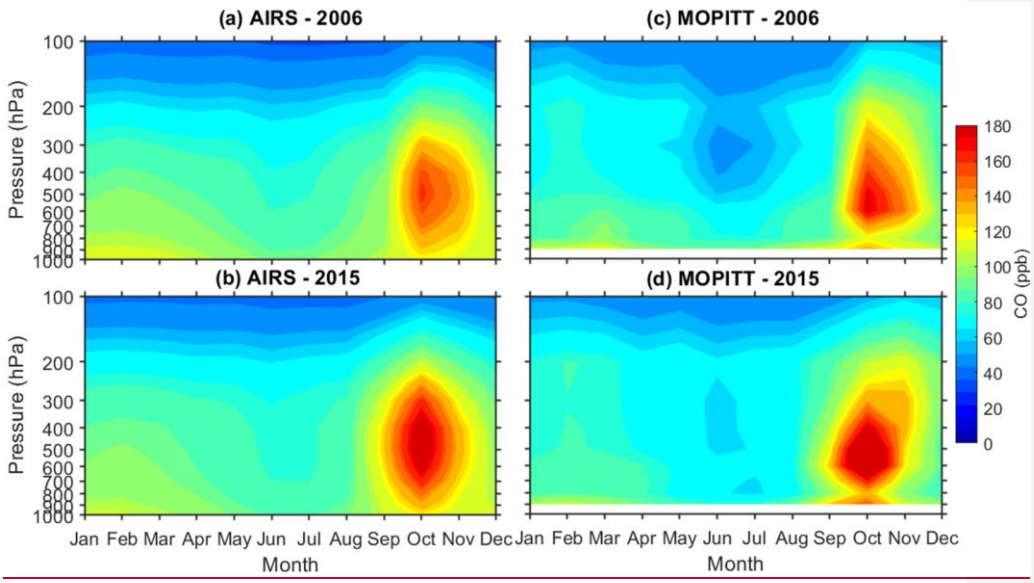

Figure 3. Pressure-time cross-section of monthly mean carbon monoxide observed over the Maritime continent (average over 90E-140E,10S-10N) in (a) 2006, (b) 2015 obtain from AIRS satellite measurements. Subplots (c) and (d) are the same as subplots (a) and (b) but for the MOPITT satellite measurements.

Formatted: Font: Bold

~~**Higher CO mixing ratios in October 2006 and 2015 at LABS**~~

Figure ~~2~~ 4 summarizes the inter-annual variations of CO in October observed at LABS along with MODIS active fire counts over Indonesia and the observed Niño 3.4 and the IOD index values, which helped to motivate this study. The highest CO mixing ratios for this period were observed in 2006 and 2015, well over the long-term means of 132.1±23.3ppb when including all points and 126.8±19.6 ppb when excluding 2006 and 2015. A significant enhancement of CO, over the latter mean calculation, of more than 47.2 ppb (37.2%) in 2006 and 36.7 ppb (28.9%) in 2015 was observed, with the value in 2006 (2015) more significant than the ±2σ (±1σ) standard deviation of the long-term mean (**Table 1**). Higher CO mixing ratios in 2006 and 2015 at LABS were also evident from the MOPITT and AIRS satellite measurements obtained over a 1-degree radius around the LABS location (Sup. **Fig.** ~~3~~1).

Unprecedented CO values in 2006 and 2015 at LABS could be due to the transport of CO from large-scale forest fires that were intense during the same period in the Indonesian ~~region~~ region. It is clear from **Figure ~~2~~4**, that the higher values of CO at LABS in 2006 and 2015 coincided with more intense fire activity over Indonesia along with warm phases of ENSO and IOD (**Fig. ~~2c~~ 4c and ~~2d~~4d**), which have been extensively studied due to the induced drought conditions in those years (Field et al., 2016; Huijnen et al., 2016; Pan et al., 2018). Previous studies (e.g., Logan et al., 2008; Zhang et al., 2011; Field et al., 2016; Pan et al., 2018) have demonstrated the direct relationship between strong Indonesian fires and El Niño events. ~~Several studies have reported on the impact of the intense BB in 2006 and 2015 on the release of significant carbon emissions and the air quality over the wider Equatorial Asian region (Logan et al., 2008; Chandra et al., 2009; Field et al., 2016; Huijnen et al., 2016; Ravindra Babu et al., 2019).~~ . The enhanced CO values from the 2006 and 2015 events at LABS in the present study complement the findings of Matsueda and Inoue (1999) in the case the of 1997 El Niño event and Nara et al. (2011) in the case of 2006 El Niño event. However, the impact on CO at LABS occurred significantly further north of the source region than in either of the aforementioned studies. Based on aircraft measurements, Matsueda and Inoue (1999) reported the enhancement of CO_2, CO, and CH_4 in the upper troposphere (at 9-12 km) over the South China Sea (SCS) during October 1997 Indonesian fire event. However, this large CO increase appeared only over the SCS west of Kalimantan and not in the subtropics between 10°N and 26°N. Nara et al. (2011) reported a substantial increase in CO mixing ratios over the Western Tropical Pacific Ocean (between 15°N and the Equator) by shipboard observations routinely operated between Japan and Australia and New Zealand during October and November of 2006. Similarly, Pochanart and Akimoto (2003) also reported the influence of the 1997 Indonesian fire event on CO enhancement at the rural station Srinakarin (14°220N, 99°070E, 296 m above sea level) in Thailand.

In addition, due to La Niña and the negative phase IOD, the fire activity in Indonesia during 2016 was much less intense than in 2006 and 2015 (**Fig. ~~2c~~ 4c** and **~~2d~~4d**). Interestingly, CO at LABS during 2016 exhibited the lowest October values in the entire data period, ~39.8 ppb (31.4%) lower than the long-term October mean (2006-2021). It is well known that the major sources of CO at LABS are BB from peninsular SEA in spring and industrial emissions from continental Asia in winter (Ou-Yang et al., 2014; Pani et al., 2019; Ravindra Babu et al., 2022; Ou-Yang et al., 2022). However, October is a transition month from the summer to winter at

LABS, when air masses can still arrive from the Pacific Ocean. Our analysis (**Fig. ~~2~~4**) suggests that the extensive fires that occurred during the 2006 and 2015 El Niño events over Indonesia may have yielded the unprecedented CO mixing ratios at LABS in October of those years. Combined El Niño and IOD-related changes in the large-scale dynamics and circulations may have promoted CO emissions from Indonesian fires to transport to LABS.

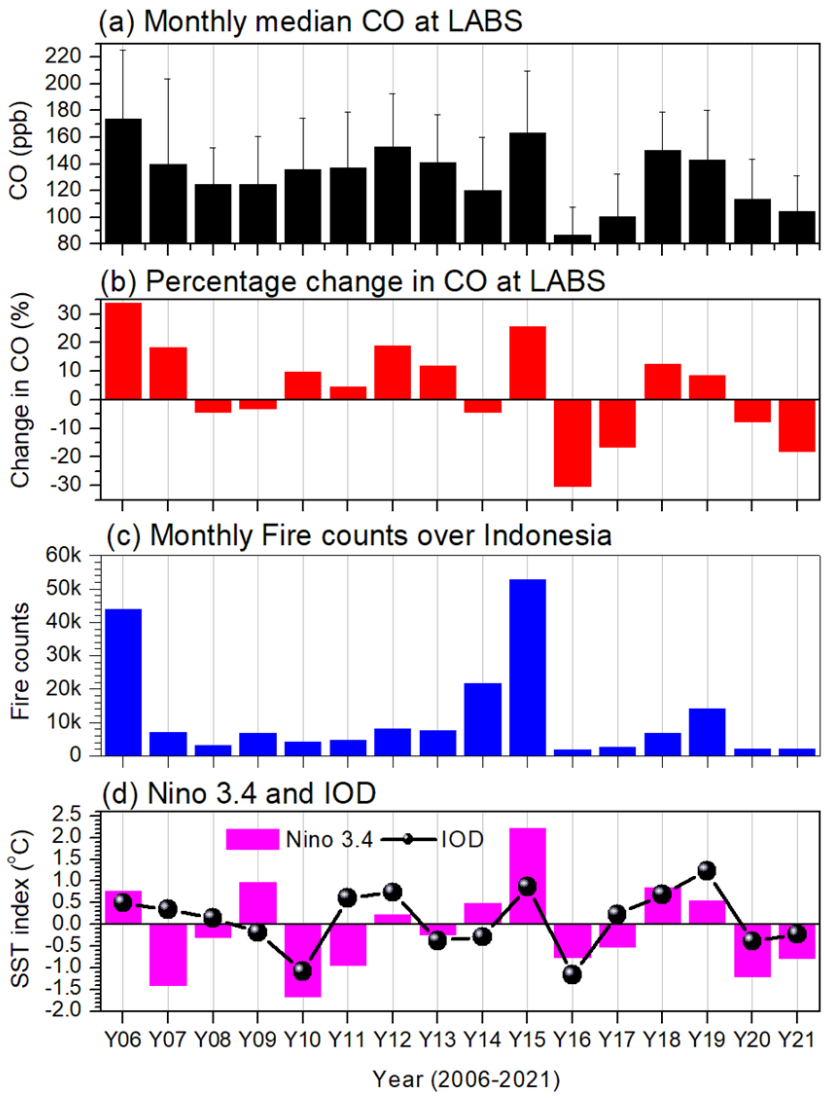

Figure ~~2~~4. Inter-annual variations in October of the (a) monthly median of CO, (b) percentage change in CO from the long-term mean at LABS, (c) MODIS (Moderate Resolution Imaging Spectroradiometer) total active fire counts (only fires tagged with >30 % confidence) over

Indonesia, (d) sea surface temperature index for Niño 3.4 (magenta) and Indian ocean dipole (black) during 2006 to 2021.

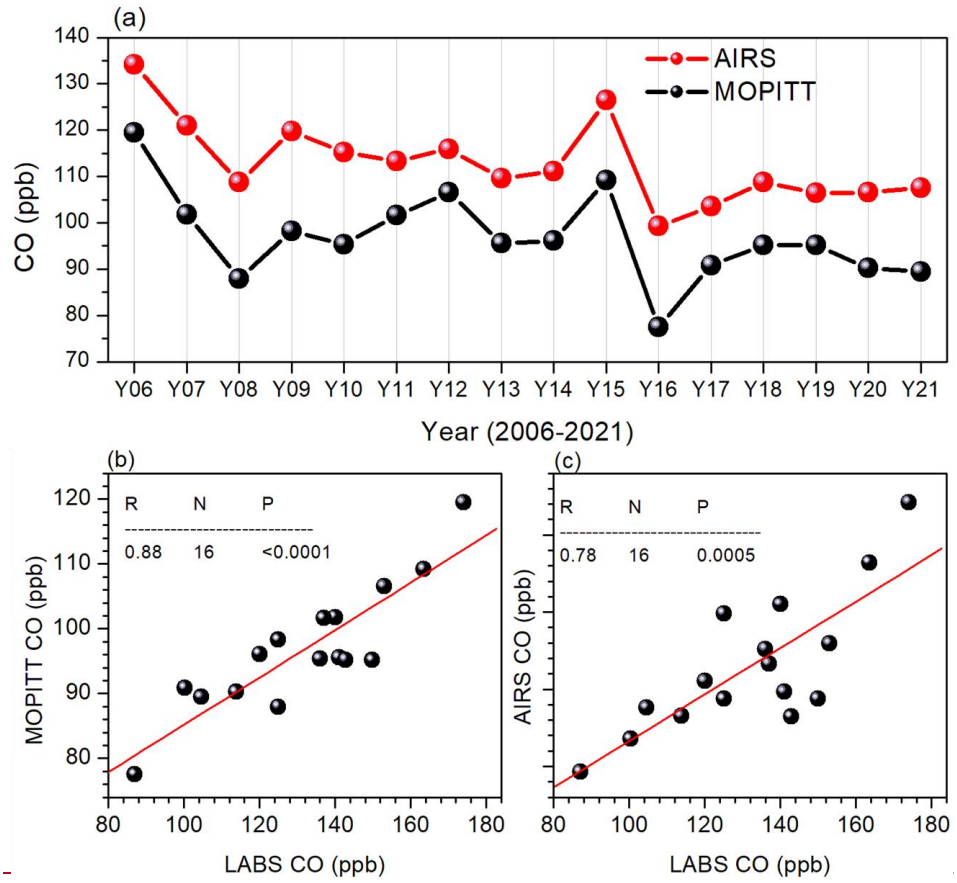

Figure 3. (a) MOPITT (black) and AIRS (red) satellite observed CO mixing ratios within the 1-degree radius around the LABS location, (b) correlation plot between in-situ CO at LABS and MOPITT CO, and (c) correlation plot between in-situ CO at LABS and AIRS CO in October month during 2006 to 2021. (R is the correlation coefficient; N is the sample size; P is the significance value)

To confirm the impact of Indonesian fire pollution on LABS CO, we further checked the spatial distribution of CO in 2006 and 2015 from the MOPITT satellite CO observations. An inter-comparison between October monthly mean CO at LABS (2006-2021) and MOPITT and AIRS CO data at 700 hPa within the 1-degree radius around the LABS location yielded correlation coefficients of 0.88 and 0.78 ($p<0.01$), respectively (Sup. **Fig. ~~3~~2**). We then used the MOPITT satellite data to track the spatial and vertical CO changes in October 2006 and 2015; first, we examined the distribution of the CO anomalies at free tropospheric heights in those years. **Figure ~~4~~ 5** shows these anomalies compared to the long-term mean (2001-2021) at 700 hPa and 500 hPa, revealing extensive enhancements of CO mixing ratios over most of equatorial Asia in 2006 and 2015. **Figure ~~4~~ 5** indicates that CO from the Indonesian fires affected both the Indian Ocean to the west and South Pacific and the northern Pacific to the east. Furthermore, these outflows of CO split northwestward into the Bay of Bengal and northeastward into the western North Pacific. It is also worth noting that the anomalies were significantly higher at 500 hPa than 700 hPa. Elevated CO is visible in the Taiwan region at 700 hPa and 500 hPa in both years. This further provides a clear signature of the impact of Indonesian fire activity on enhanced CO in 2006 and 2015 at LABS. Overall, from **Figure ~~4~~5**, MOPITT CO data shows the Indonesia fires transported CO vertically and horizontally in all directions. We further investigated the associated dynamics and large-scale circulations supporting the transport of Indonesian pollution to LABS.

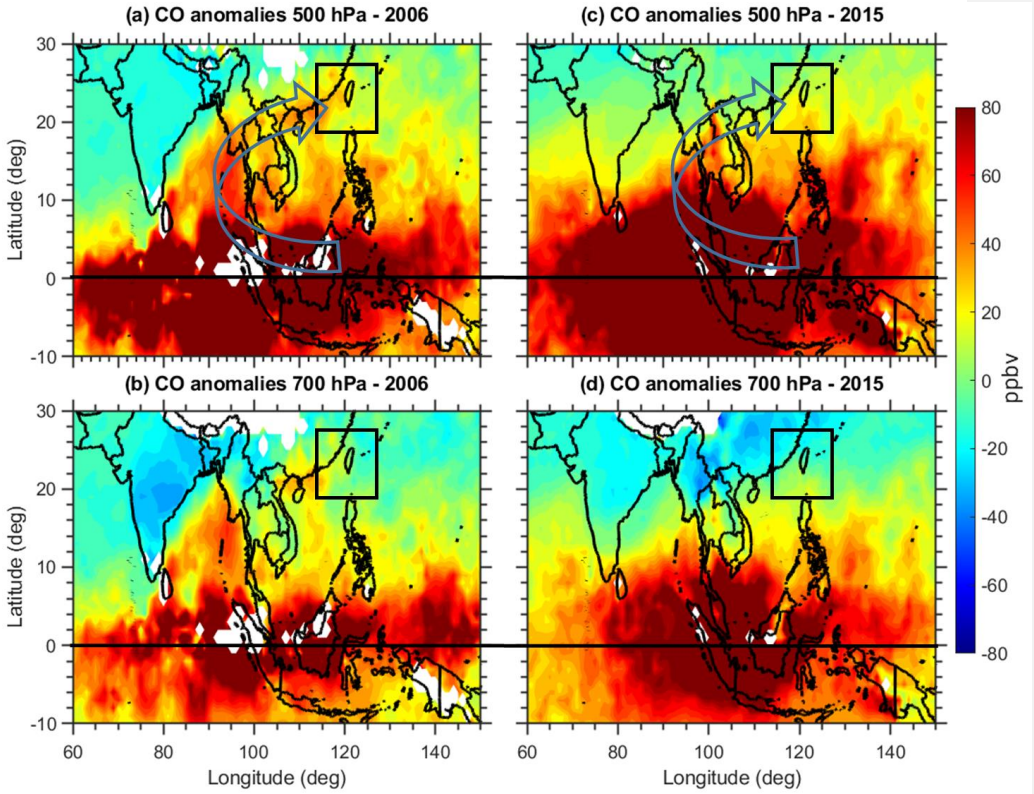

Figure 4~~5~~. Monthly mean CO anomalies obtained from MOPITT satellite observations (a) at 500 hPa and (b) at 700 hPa during October 2006. Subplots (c) and (d) are the same as subplots (a) and (b) but for October 2015, respectively. The anomalies are obtained by subtracting the 2006 and 2015 data from the long-term mean of MOPITT CO data from ~~2001 to~~2001 to 2021.

3.2 Role of large-scale dynamics and atmospheric circulations

Large-scale dynamics and circulations can play a crucial role in transporting Indonesian pollution to long-distance downwind regions (Bowman, 2006; Nara et al., 2011; Matsueda et al., 2019). To understand the plausible mechanisms behind the transport of Indonesian fire pollution to LABS, we further examined the MERRA-2 reanalysis of geopotential height (GpH) and wind distribution in 2006 and 2015. The spatial distribution of GPH at two pressure levels (700 and 500 hPa) in both events is shown in **Figure ~~5~~6**. The GpH and wind vectors in the two event years

exhibited quite different patterns in relation to a high-pressure system over the northern parts of the SCS. A high-pressure anti-cyclonic circulation center extended from the Indo-China Peninsula to the SCS in October 2006 with LABS located precisely on the eastern edge of the anticyclone. In 2015, the anticyclone extended from the Indo-China Peninsula to the western North Pacific region and over Taiwan.

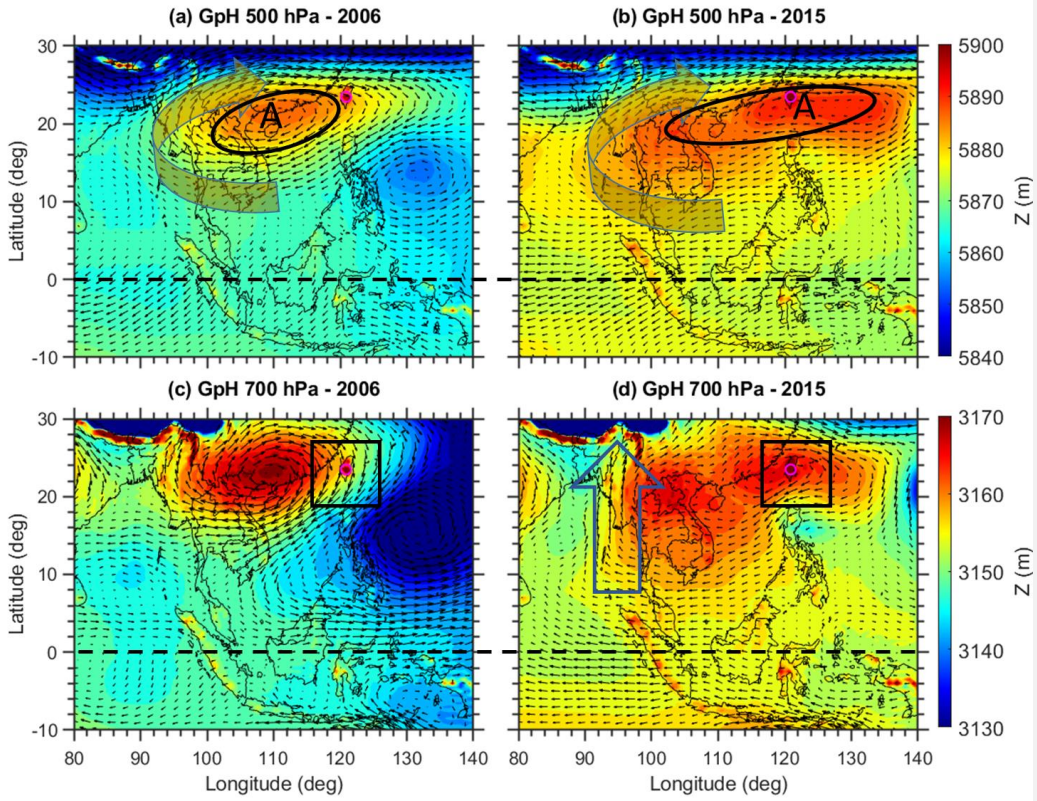

Figure ~~5~~6. Monthly mean Geopotential height (GpH) obtained from MERRA-2 reanalysis (a) at 500 hPa and (b) at 700 hPa during October 2006. Subplots (c) and (d) are the same as subplots (a) and (b) but for October 2015.

During both event years, strong southerlies at 500 hPa were evident due to the high-pressure anticyclone system in the northern SCS. It is assumed that the northern edge of the Indonesian fire pollution plume can be carried out by the southerlies and around the western edge

of the high-pressure anti-cyclone over SCS. An apparent merging of the southerlies from the equator with the subtropical westerlies in the northern PSEA region subsequently led to the transport of CO to downwind LABS. Overall, in both events, there was a significant anticyclone over the SCS. El Niño and the positive IOD-induced high-pressure anticyclone over SCS strengthen the southerlies from the equator, consequently bringing higher amounts of CO to LABS. We further investigated the vertical pressure velocity (omega) behavior in both events (Sup. Fig 3~~**Fig. 6**~~**)**, where negative (positive) values represent upward (downward) winds. Significant upward wind in both events was evident over equatorial MC, while vertical pressure velocity over Taiwan and surrounding regions at both pressure levels were mostly downwards in 2006 and 2015. The presence of a downwind will provide downward transport of any pollutant presence in the upper troposphere over that region. Also, the downward wind was relatively higher in 2006 compared to 2015. The center of the downward wind was shifted eastwards in the western North Pacific in 2015. The distinct behavior of vertical pressure velocity ~~at~~ around ~~the~~ LABS ~~region~~ during these two events might be due to the associated climate conditions in the two periods; more discussion will be provided in section 3.4.

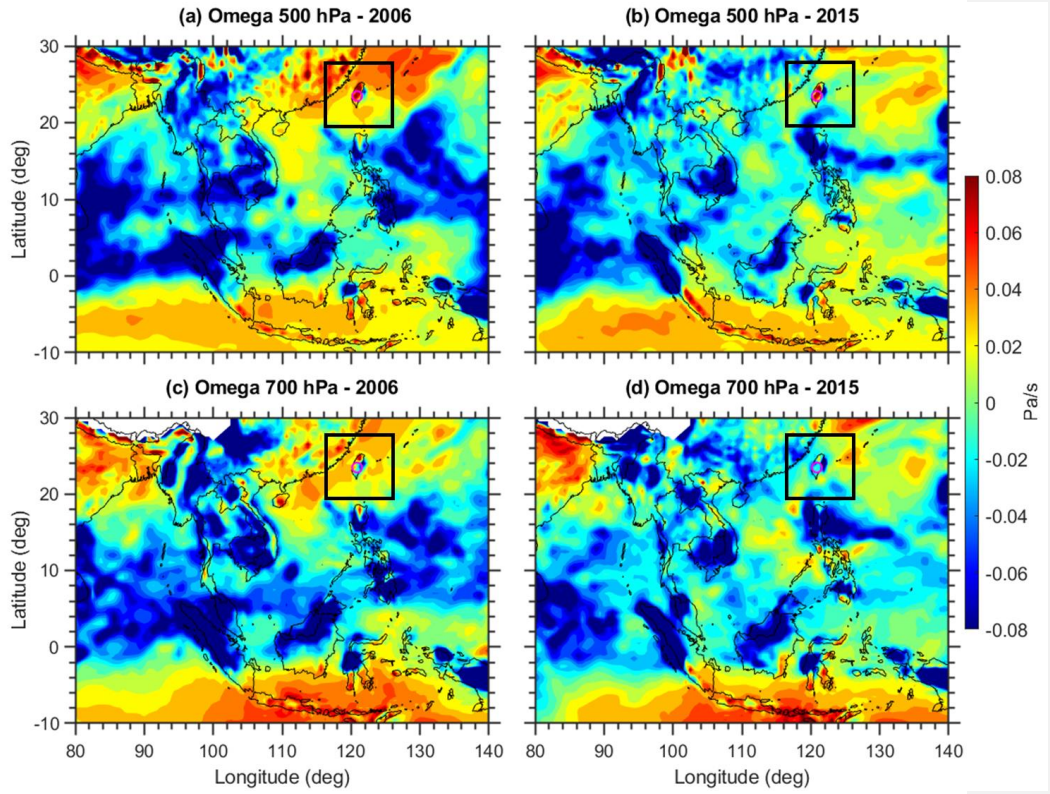

~~**Figure 6.** Monthly mean vertical pressure velocity obtained from MERRA-2 reanalysis (a) at 500 hPa and (b) at 700 hPa during October 2006. Subplots (c) and (d) are the same as subplots (a) and (b) but for October 2015.~~

We further showed CO deviations at both pressure levels in October 2016 when there was very low fire activity in Indonesia (**Fig. ~~7~~8**). Interestingly, there was a significant lowering of CO over the Taiwan region in 2016, which agrees with the observed low CO values from the in-situ measurements at LABS **(Fig. ~~2b~~4b)**. Also in agreement, 2016 was a La Niña and negative IOD year and fire activity was much weaker (**Fig. ~~2c~~ 4c** and **~~2d~~4d**). During the La Niña years, large-scale dynamical processes are greatly reversed with respect to El Niño years. We further analyzed the GpH and wind circulation patterns in 2016 (**Fig. ~~8~~9**). A significant high-pressure system (western North Pacific subtropical High) was present over the western North Pacific region in

2016, which was shifted considerably further eastward compared to ~~over~~ the SCS in 2006 and 2015. The wind vectors also highlighted the transport of a clean marine air mass from the Pacific Ocean to LABS in 2016. Interestingly, the vertical pressure velocity exhibited a pronounced upward wind over Taiwan in 2016, in contrast to the downward wind in 2006 and 2015. This indicates that dominant clean marine air reached LABS in 2016 resulting in the lowest CO mixing ratio in the entire dataset at LABS.

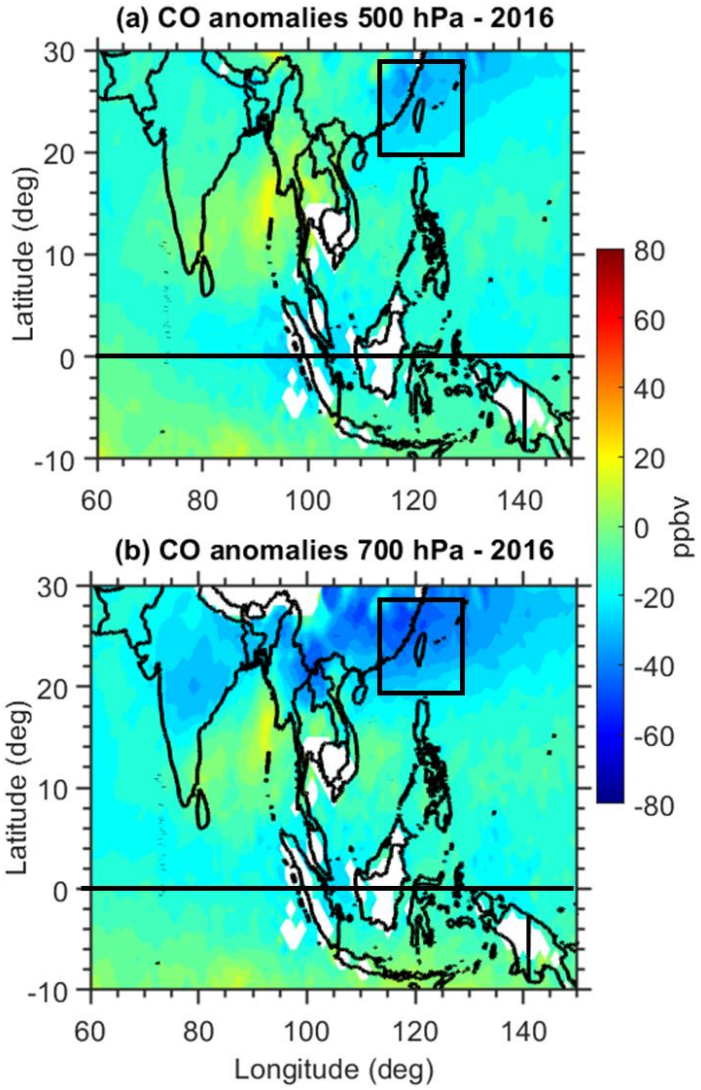

Figure ~~7~~8. Monthly mean CO deviations from the long-term mean (2001-2021) were obtained from MOPITT satellite observations (a) at 500 hPa and (b) at 700 hPa during October 2016.

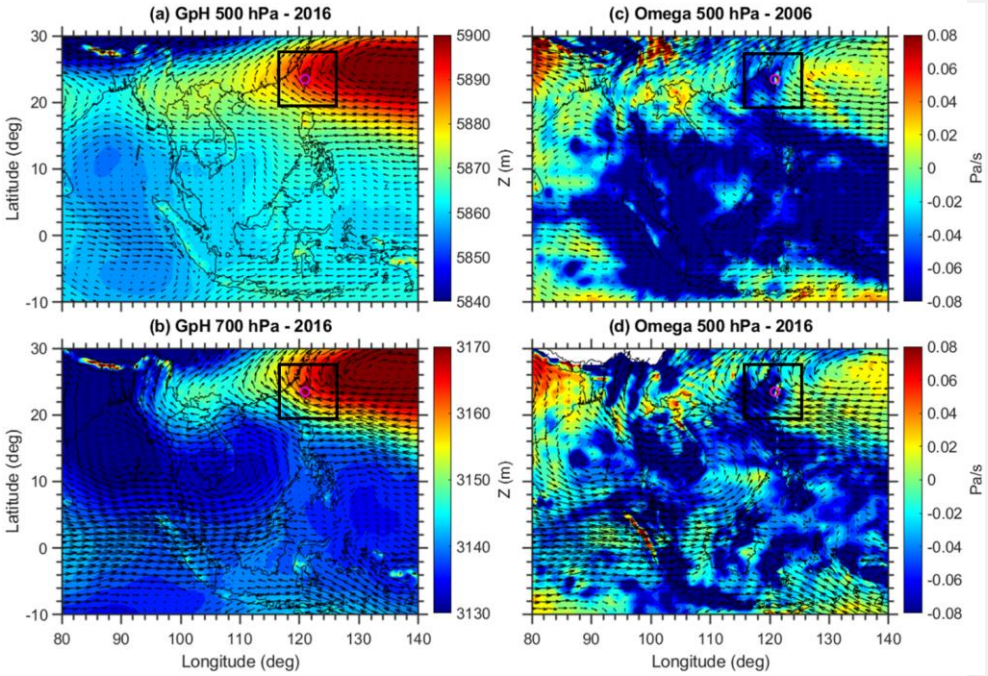

Figure ~~8~~9. Monthly mean Geopotential height (GpH) obtained from MERRA-2 reanalysis (a) at 500 hPa, and (b) at 700 hPa during October 2016. The subplots (c) and (d) are the same as subplots (a) and (b) but for the observed vertical pressure velocity (Omega).

3.4 Role of Hadley circulation

The Hadley circulation (HC) is a crucial component of the climate system, which is characterized by a thermally driven large-scale meridional circulation (Hadley, 1735). This circulation links the troposphere and stratosphere and the tropics and extra-tropics, through horizontal and vertical motions, transporting moisture, heat, and momentum to regulate Earth's energy budget. As the CO sources (Indonesia) in this study were close to the equator, it is expected that air tends to rise more or less directly over the CO sources. **Figure ~~9~~10** shows the vertical-meridional cross-section of CO and vertical pressure velocity in separate panels averaged along 110°–130°E in October 2006 and 2015. The black-colored vertical line in all the panels in **Figure ~~9~~10** shows the location of LABS and the horizontal line represents the 700 hPa. The vertical cross-section of CO highlights the uplifting of CO into the upper troposphere over the equator, followed

by southward and northward movement in both 2006 and 2015 (**Fig.** ~~**9a**~~ **10a** and ~~**9b**~~**10b**). A clear transport of CO from the source region to the sub-tropics via meridional transport was evident in both events. It is noted that the higher CO observed between 20–30°N latitude below ~700 hPa is related to anthropogenic emissions and not due to the Indonesian fires. To confirm the lofted CO from Indonesia ~~is~~ really descended in the subtropics due to the Hadley circulation, we looked into the vertical cross-section of vertical pressure velocity in both events. From **Figure** ~~**8**~~**10**, it is suggested that large amounts of CO from Indonesia were transferred into the free troposphere by the strong upward air motion in this region. Similarly, there was a pronounced descending motion (positive values of vertical pressure velocity) during October 2006 (**Fig.** ~~**9c**~~**10c**) in the northern hemisphere subtropics around 20–30°N latitude, which corresponds well with the location of LABS. However, in October 2015, the descending motion was not significant compared to 2006. This may be due to the different El Niño conditions in 2006 and 2015. While IOD conditions were indeed similar between 2006 and 2015 (**Fig.** ~~**2d**~~**4d**), the higher descending motions in 2006 can be explained in part by the moderate El Niño conditions during that year. A well-developed El Niño condition was already established in 2015 compared to 2006. In October 2006, the observed Niño 3.4 value was around 0.7 whereas in 2015 it was around 2.21. These values indicate that the El Niño conditions were already well established in October 2015 whereas, in 2006, the conditions were not developed as El Niño. It is reported that in El Niño conditions, the western Pacific HC is observed to be weakened whereas the eastern Pacific HC is strengthened (Wang, 2004). This is supported by the observed lesser descending motions in 2015 from the present study. These differences in the descending motions likely influenced the greater CO enhancement in 2006 compared to 2015 at LABS (**Fig.** ~~**2b**~~ **4b** and **Table 1**). Overall, it is clearly illustrated from the MOPITT CO vertical cross-section and the MERRA-2 vertical pressure velocity that the CO emitted from the Indonesian fire was transported vertically through the Hadley circulation to the LABS location.

Formatted: Font: Bold

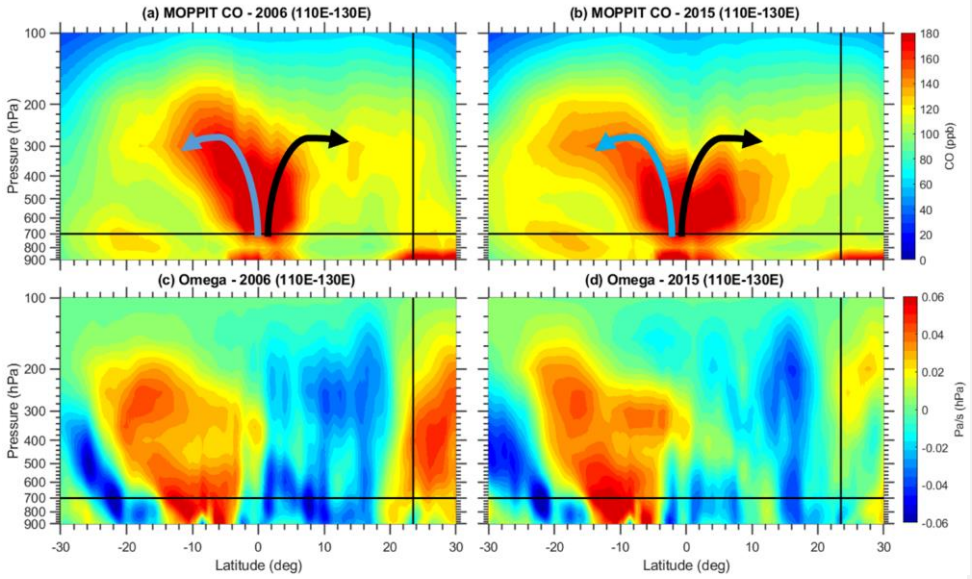

Figure ~~9~~10. ~~Vertical~~Pressure–latitude~~meridional~~ cross-section of MOPITT CO averaged along 110°–130°E (a) for October 2006 and (b) for October 2015. Subplots (c) and (d) are the same as subplots (a) and (b) but for the MERRA-2 reanalysis vertical pressure velocity. Positive (negative) values represent the downward (upward) wind.

One of the worst fire events in Indonesia's history occurred in October 1997 and was associated with an El Niño event and a positive IOD (Duncan et al., 2003a). In order to see any similarities between 1997 and 2006 and 2015, particularly in large-scale circulations, we further checked the MERRA-2 GpH and wind circulation pattern in October 1997. To note, none of the satellite measurements of CO (either AIRS or MOPITT) are available during the 1997 event, and measurements at LABS didn't start until 2006. Hence, we only cross-checked the large-scale circulations that are observed in October 1997, respectively. Sup. Figure 4a shows the spatial distribution of GpH observed at 500 hPa and Sup. Figure 4b shows the vertical-meridional cross-section of vertical pressure velocity averaged along 110°–130°E in October 1997. Interestingly, we noticed a significant high-pressure anti-cyclonic circulation over northern parts of the SCS in October 1997 as observed in 2006 and 2015. Also evident is the merging of the southerlies from the MC with the subtropical westerlies in the northern PSEA region. Similarly, the vertical

Formatted: Indent: First line: 0.5"

pressure velocity also shows the upward wind over the MC and the downward wind over the northern hemisphere subtropics around 20–30°N latitude. From Sup. Figure 4b, it is very clear that a significant descending wind was evident around the LABS location in 1997 similar to 2006 and 2015. Overall, it is very clear from the present results that it is possible to transport pollution from Indonesia to sub-tropical East Asia during extreme and higher-duration fire events like 1997, 2006, and 2015.

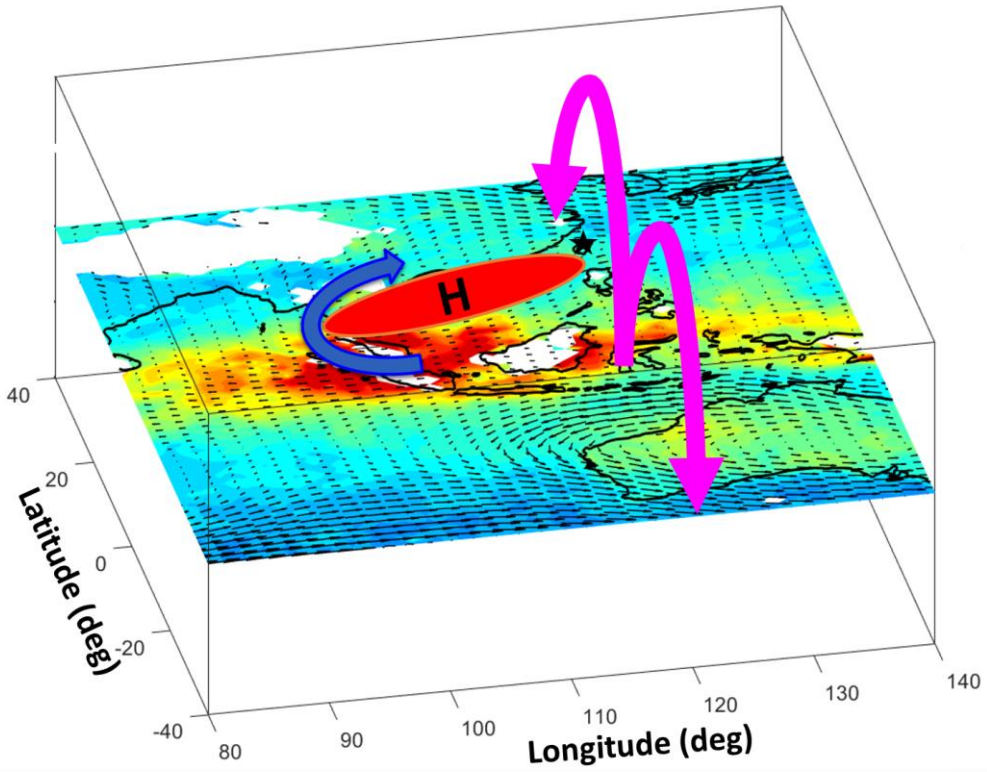

Figure 11. Schematic diagram of CO transport from Indonesian fires to subtropical East Asian region. The horizontal transport of CO due to the high-pressure anticyclone is denoted by the blue-colored arrow. H denotes a high-pressure anticyclone over northern parts of the South China Sea. Magenta-colored arrows indicate the transport of CO through the local Hadley circulation (over 110°–130°E). Black-colored star symbol represents the LABS location.

The major transport pathways of CO from Indonesia to subtropical East Asia are illustrated in a schematic diagram (Figure 11). Illustrated mechanisms include horizontal transport in the free troposphere due to El Niño and positive IOD-induced high-pressure anticyclone circulation, and vertical transport through the Hadley circulation. The southerlies on the southwest flank of the anticyclone merged with the subtropical westerlies over PSEA and then transported polluted air to LABS. Apart from this horizontal transport, CO was transported through the Hadley circulation to LABS in both events. However, there was a distinctly different Hadley Circulation strength in 2006 compared to 2015 due to the different El Niño conditions. These two events were strongly associated with positive IOD, but in 2006, the El Niño conditions were not well-developed, whereas in 2015 well-developed El Niño conditions were evident. These El Niño conditions further suppressed the HC over the western Pacific in 2015 compared to 2006. This suggested the importance of the background climate conditions (ENSO and IOD) on the pollutant transport process.

4. Summary and Conclusions

Due to the combined impact of positive phase IOD and El Niño-induced drought conditions in 2006 and 2015, Indonesia experienced extreme fire activity. MODIS active fire counts showed the largest fires in October 2006 and 2015 compared to the other years in the 16-year period in Indonesia. These record fires reflected two of the largest carbon emissions in the Indonesian region since 1997.~~– Changes in the background climate will inevitably impact meteorological transport processes and the concentrations of pollutants arriving at downwind regions.~~ Lulin Atmospheric Background Station (LABS, 23.47°N 120.87°E, 2862 m ASL) is the only high-altitude background station located in the western North Pacific region, and is optimally located to study some of these transport processes, including long-range transport of pollution in the free troposphere and stratospheric intrusions. Interestingly, during these two events (October 2006 and 2015), we noticed an abnormal enhancement of CO compared to other years at LABS from the in-situ measurements. In the present study, for the first time, the impact of Indonesia fire pollution on CO measurements at LABS and the plausible transport pathways for the transport of CO from Indonesia to sub-tropical East Asia were investigated. The main findings are summarized below:

1. Compared to 16-year (2006-2021) means, a substantial increase in CO mixing ratios of about ~47.2 ppb (37.2%) in October 2006 and ~36.7 ppb (28.9%) in October 2015 was observed at LABS.
2. By comparing the CO and atmospheric large-scale circulation data, we found two plausible transport pathways of CO from Indonesia to LABS. i.e. horizontal transport in the free troposphere and vertically through the Hadley Circulation.
3. El Niño and positive IOD-induced high-pressure anticyclone circulation over northern parts of the South China Sea play an important role in the horizontal transport of CO.
4. Distinct strength of the Hadley circulation over the western Pacific was observed in October 2006 (stronger) and 2015 (weaker). Well-developed El Niño conditions in October 2015 suppressed the strength of the Hadley Circulation over the western Pacific.

A changing warmer climate can influence carbon emissions and alter the transport pathways, hence impacting the various scales of air pollution and climate. Changes in the background climate will inevitably impact meteorological transport processes and the concentrations of pollutants arriving at downwind regions. Overall, the present results further provide knowledge to the atmospheric chemistry community about the different transport pathways of pollutants and the role of climate conditions.

~~During October 2006 and 2015, there were substantial increases in CO mixing ratios, ~47.2 ppb (37.2%) and ~36.7 ppb (28.9%) increase compared to the 16-year (2006-2021) means at LABS. Interestingly, these two events (2006 and 2015) were strongly associated with the two major biomass burning episodes over Indonesia, which resulted from a combined impact of positive phase ENSO and IOD-induced drought conditions. MODIS active fire counts showed the largest fires in October 2006 and 2015 compared to the other years in the 16-year period in Indonesia. These record fires reflected two of the largest carbon emissions in the Indonesian region since 1997. Apart from these high values in October 2006 and 2015, in October 2016, extremely low CO values were recorded at LABS (~31.4% lower compared to 2006-2021 mean). October 2016 was associated with negative IOD over the Indian Ocean and La Niña in the Pacific Ocean, resulting in the lowest fire activity over the MC. Further, we found that the large-scale circulations in 2016 were quite different from 2006 and 2015. In 2016, LABS was dominated by the southerlies~~

Formatted: Font: (Default) Times New Roman, 12 pt
Formatted: List Paragraph, Numbered + Level: 1 + Numbering Style: 1, 2, 3, … + Start at: 1 + Alignment: Left + Aligned at: 0.25" + Indent at: 0.5"
Formatted: Font: 12 pt
Formatted: Font: (Default) Times New Roman, 12 pt
Formatted: Font: (Default) Times New Roman, 12 pt
Formatted: Font: (Default) Times New Roman, 12 pt
Formatted: Font: (Default) Times New Roman, 12 pt
Formatted: Font: (Default) Times New Roman, 12 pt
Formatted: Font: (Default) Times New Roman, 12 pt
Formatted: Pattern: Clear
Formatted: Indent: First line: 0"
Formatted: Font: (Default) Times New Roman, 12 pt

due to the western Pacific subtropical High (WPSH), which transported clean marine air from the Pacific Ocean and caused record-low CO values at LABS. The main aim of our study was to examine the transport pathways of CO from Indonesia's source region to the downwind LABS region. By comparing the CO and atmospheric circulation data from the 2006 and 2015 El Niño (positive IOD) years and 2016 La Niña (negative IOD), we found two plausible transport pathways of CO from Indonesia to LABS.

Figure 10 illustrates a schematic diagram of the major transport pathways of CO from Indonesia to subtropical East Asia during the two event years. They include horizontal transport in the free troposphere due to El Niño-induced high-pressure anticyclone circulation and vertically through the Hadley circulation. For October 2006 and 2015, corresponding to El Niño and positive IOD, northern SCS was influenced by the high-pressure anti-cyclonic system in the free troposphere. The southerlies on the southwest flank of the anticyclone further merged with the subtropical westerlies over PSEA and then transported polluted air to LABS. Apart from this horizontal transport, CO was transported through the Hadley circulation to LABS in both events. However, there was a distinctly different HC strength in 2006 compared to 2015 due to the different El Niño conditions. These two events were strongly associated with positive IOD, but in 2006, the El Niño conditions were not well developed, whereas in 2015 well-developed El Niño conditions were evident. These El Niño conditions further suppressed the HC over the western Pacific in 2015 compared to 2006. This suggested the importance of the background climate conditions (ENSO and IOD) on the pollutant transport process. A changing warmer climate can influence carbon emissions and alter the transport pathways, hence impacting the various scales of air pollution and climate. Overall, the present results further provide knowledge to the atmospheric chemistry community about the different transport pathways of pollutants and the role of climate conditions.

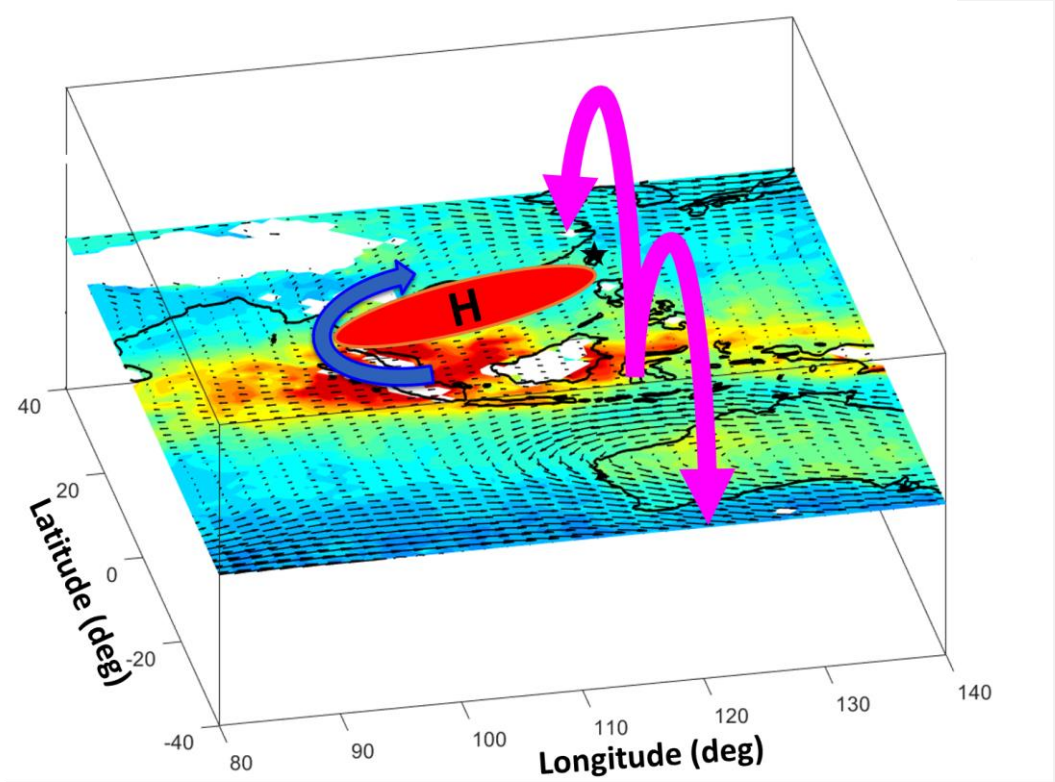

~~**Figure 10.** Schematic diagram of CO transport from Indonesian fires to subtropical East Asian region. Horizontal transport of CO due to the high-pressure anticyclone is denoted by the blue-colored arrow. H denotes high-pressure anticyclone over northern parts of the South China Sea. Magenta-colored arrows indicate the transport of CO through the local Hadley circulation (over 110°–130°E). Black-colored star symbol represents the LABS location.~~

Data availability

The CO data at LABS can be assessed at http://lulin.tw/index_en.htm. The AIRS and MOPITT CO data can be downloaded from the following websites https://disc.gsfc.nasa.gov/datasets/AIRS3STM_7.0 (AIRS project., 2019) and https://asdc.larc.nasa.gov/project/MOPITT. MERRA-2 data are available online through the

NASA Goddard Earth Sciences Data Information Services Center (GES DISC; https://disc.gsfc.nasa.gov, last access: 30 May 2022). Nino 3.4 Index and IOD data can be downloaded through the following websites https://psl.noaa.gov/gcos_wgsp/Timeseries/Niño34/. https://psl.noaa.gov/gcos_wgsp/Timeseries/DMI/. The MODIS fire products can be downloaded from the following website https://firms.modaps.eosdis.nasa.gov/active_fire/.

Author contributions

Saginela Ravindra Babu: Conceptualization, Data curation, Formal analysis, Investigation, Software, Validation, Visualization, Writing – original draft preparation, Writing – review and editing; **Chang-Feng Ou-Yang**: Data curation, Software, Validation, Visualization; **Stephen M. Griffith**; Writing – review and editing; **Shantanu Kumar Pani**: Data curation and Visualization; **Steven S. Kong**: Data curation and Visualization; **Neng-Huei Lin**: Conceptualization, Investigation, Funding Acquisition, Supervision, Resources, Writing – review and editing.

Competing Interest

The authors declare that they have no conflict of interest.

Acknowledgments

The work is primarily supported by the Ministry of Science and Technology, Taiwan under the grants of MOST 110-2811-M-008-562 and MOST 109-2811-M-008-553. Authors thanks to Taiwan Environmental Protection Administration (TEPA) for supporting the air pollutants monitoring at LABS. The authors thank NASA and NOAA for providing MOPITT, MODIS, and AIRS satellite data. We thank NASA's Global Monitoring and Assimilation Office (GMAO) for providing the Modern-Era Retrospective analysis for Research and Applications, Version 2 (MERRA-2) data. We also thank NOAA ESRL Physical Sciences Laboratory for providing Indian Ocean Dipole and Niño 3.4 index values through the following websites https://psl.noaa.gov/gcos_wgsp/Timeseries/DMI/ https://psl.noaa.gov/gcos_wgsp/Timeseries/Niño34/.

5. References

AIRS project (2019), Aqua/AIRS L3 Monthly Standard Physical Retrieval (AIRS-only) 1-degree x 1 degree V7.0, Greenbelt, MD, USA, Goddard Earth Sciences Data and Information Services Center (GES DISC), Accessed: (11 September 2022), 10.5067/UBENJB9D3T2H.

Bowman, K. P. and Cohen, P. J.: Interhemispheric exchange by seasonal modulation of the Hadley circulation, J. Atmos. Sci., 54, 2045–2059, https://doi.org/10.1175/1520-0469(1997)054%3C2045:IEBSMO%3E2.0.CO;2, 1997.

Bowman, K. P.: Transport of carbon monoxide from the tropics to the extratropics, J. Geophys. Res.-Atmos., 111, https://doi.org/10.1029/2005JD006137, 2006.

Chandra, S., Ziemke, J. R., Duncan, B. N., Diehl, T. L., Livesey, N. J. and Froidevaux, L.: Effects of the 2006 El Niño on tropospheric ozone and carbon monoxide: implications for dynamics and biomass burning, Atmos. Chem. Phys., 9, 4239–4249, https://doi.org/10.5194/acp-9-4239-2009, 2009.

Chandra, S., Ziemke, J. R., Schoeberl, M. R., Froidevaux, L., Read, W. G., Levelt, P.F. and Bhartia, P. K.: Effects of the 2004 El Nino on tropospheric ozone and water vapor, Geophys.Res. Lett., 34, L06802, https://doi.org/10.1029/2006GL028779, 2007.

Chi, K.H., Hung, N.T., Lin, C.Y., Wang, S.H., Ou-Yang, C.F., Lee, C.T. and Lin, N.H.: Evaluation of Atmospheric PCDD/Fs at Two High-Altitude Stations in Vietnam and Taiwan during Southeast Asia Biomass Burning. Aerosol Air Qual. Res. 16: 2706-2715. https://doi.org/10.4209/aaqr.2015.11.0653, 2016.

Chuang, M. T., Fu, J. S., Lee, C. Te, Lin, N. H., Gao, Y., Wang, S. H., Sheu, G. R., Hsiao, T. C., Wang, J. L., Yen, M. C., Lin, T. H. and Thongboonchoo, N.: The simulation of long-range transport of biomass burning plume and short-range transport of anthropogenic pollutants to a mountain observatory in east Asia during the 7-SEAS/2010 Dongsha experiment, Aerosol Air Qual. Res., 16(11), 2933–2949, https://doi.org/10.4209/aaqr.2015.07.0440, 2016.

Cheng, F.-Y., Yang, Z.-M., Ou-Yang, C.-F. and Ngan, F.: A numerical study of the dependence of long-range transport of CO to a mountain station in Taiwan on synoptic weather patterns

555 during the Southeast Asia biomass-burning season, Atmos. Environ., 78, 277–290,
556 https://doi.org/10.1016/j.atmosenv.2013.03.020, 2013.

557 Cooper, O. R., Gao, R. S., Tarasick, D., Leblanc, T., and Sweeney, C.: Long-term ozone trends at
558 rural ozone monitoring sites across the United States, 1990–2010, J. Geophys. Res.-
559 Atmos.,117, 1990–2010, https://doi.org/10.1029/2012JD018261, 2012.

560 Deeter, M. N., Edwards, D. P., Francis, G. L., Gille, J. C., Mao, D., Martínez-Alonso, S., Worden,
561 H. M., Ziskin, D., and Andreae, M. O.: Radiance-based retrieval bias mitigation for the
562 MOPITT instrument: the version 8 product, Atmos. Meas. Tech., 12, 4561–4580,
563 https://doi.org/10.5194/amt-12-4561-2019, 2019.

564 Doherty, R. M., Stevenson, D. S., Johnson, C. E., Collins, W. J., and Sanderson, M. G.:
565 Tropospheric ozone and El Nino-Southern Oscillation: Influence of atmospheric dynamics,
566 biomass burning emissions, and future climate change, J. Geophys. Res., 111, D19304,
567 https://doi.org/10.1029/2005JD006849, 2006.

568 Duncan, B. N., Bey, I., Chin, M., Mickley, L. J., Fairlie, T. D., Martin, R. V., and Matsueda, H.:
569 Indonesian wildfires of 1997: Impact on tropospheric chemistry, J. Geophys. Res., 108, 4458,
570 https://doi.org/10.1029/2002JD003195, 2003a.

571 Duncan, B. N., Martin, R. V., Staudt, A., et al.: Inter-annual and seasonal variability of biomass
572 burning emissions constrained by satellite observations, J. Geophys. Res., 108, 4100,
573 https://doi.org/10.1029/2002JD002378, 2003b.

574 Field, R. D., van der Werf, G. R., and Shen, S. S. P.: Human amplification of drought-induced
575 biomass burning in Indonesia since 1960, Nature Geoscience, 2, 185–188,
576 https://doi.org/10.1038/ngeo443,2009.

577 Field, R. D., van der Werf, G. R., Fanin, T., Fetzer, E. J., Fuller, R., Jethva, H., Levy, R., Livesey,
578 N. J., Luo, M., Torres, O., and Worden, H. M.: Indonesian fire activity and smoke pollution in
579 2015 show persistent nonlinear sensitivity to El Ni˜no-induced drought, Proceedings of the
580 National Academy of Sciences, 113, 9204–9209, https://doi.org/10.1073/pnas.1524888113,
581 2016.

582 Gelaro, R., McCarty, W., Suárez, M. J., Todling, R., Molod, A., Takacs, L., Randles, C. A.,
583 Darmenov, A., Bosilovich, M. G., Reichle, R., Wargan, K., Coy, L., Cullather, R., Draper, C.,
584 Akella, S., Buchard, V., Conaty, A., Silva, A. M. da, Gu, W., Kim, G.-K., Koster, R., Lucchesi,
585 R., Merkova, D., Nielsen, J. E., Partyka, G., Pawson, S., Putman, W., Rienecker, M., Schubert,
586 S. D., Sienkiewicz, M., and Zhao, B.: The Modern-Era Retrospective Analysis for Research
587 and Applications, Version 2 (MERRA-2), J. Climate, 30, 5419–5454,
588 https://doi.org/10.1175/jcli-d-16-0758.1, 2017.

589 Giglio, L., Schroeder, W., and Justice, C. O.: The collection 6 MODIS active fire detection
590 algorithm and fire products, Remote Sens. Environ., 178, 31–41,
591 https://doi.org/10.1016/j.rse.2016.02.054, 2016.

592 Hadley, G.: Concerning the cause of the general trade-winds. Philos. Trans. R. Soc. Lond. 29, 58–
593 62. https://doi.org/10.1098/rstl.1735.0014, 1735.

594 Heymann, J., Reuter, M., Buchwitz, M., Schneising, O., Bovensmann, H., Burrows, J. P., Massart,
595 S., Kaiser, J. W., and Crisp, D.: CO2 emission of Indonesian fires in 2015 estimated from
596 satellite-derived atmospheric CO2 concentrations, Geophys. Res. Lett., 44, 1537–1544,
597 https://doi.org/10.1002/2016gl072042, 2017.

598 Hsiao, T. C., Ye, W. C., Wang, S. H., Tsay, S. C., Chen, W. N., Lin, N. H., Lee, C. Te, Hung, H.
599 M., Chuang, M. T., and Chantara, S.: Investigation of the CCN activity, BC and UVBC mass
600 concentrations of biomass burning aerosols during the 2013 BASELInE campaign, Aerosol Air
601 Qual. Res., 16, 2742–2756, https://doi.org/10.4209/aaqr.2015.07.0447, 2016.

602 Huang, L., Lin, W., Li, F., Wang, Y. and Jiang, B.: Climate Impacts of the Biomass Burning in
603 Indochina on Atmospheric Conditions over Southern China. Aerosol Air Qual. Res. 19: 2707-
604 2720. https://doi.org/10.4209/aaqr.2019.01.0028, 2019.

605 Huang, H. Y., Wang, S. H., Huang, W. X., Lin, N. H., Chuang, M. T., da Silva, A. M. and Peng,
606 C. M.: Influence of Synoptic-Dynamic Meteorology on the Long-Range Transport of Indochina
607 Biomass Burning Aerosols, J. Geophys. Res. Atmos., 125(3),
608 https://doi.org/10.1029/2019JD031260, 2020.

609 Huijnen, V., Wooster, M. J., Kaiser, J. W., Gaveau, D. L. A., Flemming, J., Parrington, M., Inness,
610 A., Murdiyarso, D., Main, B., and van Weele, M.: Fire carbon emissions over maritime
611 southeast Asia in 2015 largest since 1997, Sci. Rep., 6, 26886,
612 https://doi.org/10.1038/srep26886, 2016.

613 Lin, C.-Y., Hsu, H.-m., Lee, Y. H., Kuo, C. H., Sheng, Y.-F., and Chu, D. A.: A new transport
614 mechanism of biomass burning from Indochina as identified by modeling studies, Atmos.
615 Chem. Phys., 9, 7901–7911, https://doi.org/10.5194/acp-9-7901-2009, 2009.

616 Lin, N.-H., Tsay, S.-C., Maring, H. B., Yen, M.-C., Sheu, G.-R., Wang, S.-H., Chi, K. H., Chuang,
617 M.-T., Ou-Yang, C.-F., Fu, J. S., Reid, J. S., Lee, C.-T., Wang, L.-C., Wang, J.-L., Hsu, C. N.,
618 Sayer, A. M., Holben, B. N., Chu, Y.-C., Nguyen, X. A., Sopajaree, K., Chen, S.-J., Cheng, M.-
619 T., Tsuang, B.-J., Tsai, C.-J., Peng, C.-M., Schnell, R. C., Conway, T., Chang, C.-T., Lin, K.-
620 S., Tsai, Y. I., Lee, W.-J., Chang, S.-C., Liu, J.-J., Chiang, W.-L., Huang, S.-J., Lin, T.-H. and
621 Liu, G.-R.: An overview of regional experiments on biomass burning aerosols and related
622 pollutants in Southeast Asia: From BASE-ASIA and the Dongsha Experiment to 7-SEAS,
623 Atmos. Environ., 78, 1–19, https://doi.org/10.1016/j.atmosenv.2013.04.066, 2013.

624 Lin, C. C., Chen, W. N., Loftus, A. M., Lin, C. Y., Fu, Y. T., Peng, C. M. and Yen, M. C.:
625 Influences of the long-range transport of biomass-burning pollutants on surface air quality
626 during 7-SEAS field campaigns, Aerosol Air Qual. Res., 17(10), 2595–2607,
627 https://doi.org/10.4209/aaqr.2017.08.0273, 2017.

628 Logan, J. A., Megretskaia, I., Nassar, R., Murray, L. T., Zhang, L., Bowman, K. W., Worden, H.
629 M., and Luo, M.: Effects of the 2006 El Niño on tropospheric composition as revealed by data
630 from the Tropospheric Emission Spectrometer (TES), Geophys. Res. Lett., 35, 1–5,
631 https://doi.org/10.1029/2007GL031698, 2008.

632 Matsueda, H. and Inoue, H. Y.: Aircraft measurements of trace gases between Japan and Singapore
633 in October of 1993, 1996, and 1997, Geophys. Res. Lett., 26, 2413–2416,
634 https://doi.org/10.1029/1999GL900089, 1999.

635 Matsueda, H., Inoue, H. Y., and Ishii, M.: Aircraft observation of carbon dioxide at 8–13 km
636 altitude over the western Pacific from 1993 to 1999, Tellus B, 54, 1–21,
637 https://doi.org/10.1034/j.1600-0889.2002.00304.x, 2002.

638 Matsueda, H., Buchholz, R. R., Ishijima, K., Worden, H. M., Hammerling, D., and Machida, T.:
639 Interannual Variation of Upper Tropospheric CO over the Western Pacific Linked with
640 Indonesian Fires, SOLA, 15, 205–210, https://doi.org/10.2151/sola.2019-037, 2019.

641 Nara, H., Tanimoto, H., Nojiri, Y., Mukai, H., Zeng, J., Tohjima, Y., and Machida, T.: CO
642 emissions from biomass burning in South-east Asia in the 2006 El Nino year: shipboard and
643 AIRS satellite observations, Environ. Chem., 8, 213–223, https://doi.org/10.1071/EN10113,
644 2011.

645 Nassar, R., Logan, J. A., Megretskaia, I. A., Murray, L. T., Zhang, L., and Jones, D. B. A.: Analysis
646 of tropical tropospheric ozone, carbon monoxide, and water vapor during the 2006 El Niño
647 using TES observations and the GEOS Chem model, J. Geophys. Res.-Atmos., 114, D17304,
648 https://doi.org/10.1029/2009JD011760, 2009.

649 Niwa, Y., Sawa, Y., Nara, H., Machida, T., Matsueda, H., Umezawa, T., Ito, A., Nakaoka, S.-I.,
650 Tanimoto, H., and Tohjima, Y.: Estimation of fire-induced carbon emissions from Equatorial
651 Asia in 2015 using in situ aircraft and ship observations, Atmos. Chem. Phys., 21, 9455–9473,
652 https://doi.org/10.5194/acp-21-9455-2021, 2021.

653 Ou-Yang, C. F., Lin, N. H., Lin, C. C., Wang, S. H., Sheu, G. R., Lee, C. Te, Schnell, R. C., Lang,
654 P. M., Kawasato, T. and Wang, J. L.: Characteristics of atmospheric carbon monoxide at a high-
655 mountain background station in East Asia, Atmos. Environ., 89, 613–622,
656 https://doi.org/10.1016/j.atmosenv.2014.02.060, 2014.

657 Ou-Yang, C. F., Ravindra Babu, S., Jia-Ren Lee, Ming-Cheng Yen, Stephen M. Griffith, Chia-
658 Ching Lin, Shuenn-Chin Chang and Neng-Huei Lin.: Detection of stratospheric intrusion events
659 and their role in ozone enhancement at a mountain background site in sub-tropical East Asia,
660 Atmos. Environ., 268, 118779, https://doi.org/10.1016/j.atmosenv.2021.118779, 2022.

661 Pani, S. K., Wang, S. H., Lin, N. H., Lee, C. Te, Tsay, S. C., Holben, B. N., Janjai, S., Hsiao, T.
662 C., Chuang, M. T. and Chantara, S.: Radiative effect of springtime biomass-burning aerosols
663 over northern Indochina during 7-SEAS/BASELInE 2013 campaign, Aerosol Air Qual. Res.,
664 16(11), 2802–2817, https://doi.org/10.4209/aaqr.2016.03.0130, 2016.

Pani, S. K., Ou-Yang, C.-F., Wang, S.-H., Ogren, J. A., Sheridan, P. J., Sheu, G.-R., and Lin, N.-H. J. A. E.: Relationship between long-range transported atmospheric black carbon and carbon monoxide at a high-altitude background station in East Asia, Atmos. Environ, 210, 86-99, https://doi.org/10.1016/j.atmosenv.2019.04.053, 2019.

Pan, X., Chin, M., Ichoku, C. M., and Field, R. D.: Connecting Indonesian fires and drought with the type of El Niño and phase of the Indian Ocean dipole during 1979–2016, J. Geophys. Res.-Atmos., 123, 1–15, https://doi.org/10.1029/2018JD028402, 2018.

Park, S., Kim, S.W., Lin, N.H., Pani, S.K., Sheridan, P.J. and Andrews, E.: Variability of Aerosol Optical Properties Observed at a Polluted Marine (Gosan, Korea) and a High-altitude Mountain (Lulin, Taiwan) Site in the Asian Continental Outflow. Aerosol Air Qual. Res. 19: 1272-1283. https://doi.org/10.4209/aaqr.2018.11.0416, 2019.

Parker, R. J., Boesch, H., Wooster, M. J., Moore, D. P., Webb, A. J., Gaveau, D., and Murdiyarso, D.: Atmospheric CH4 and CO2 enhancements and biomass burning emission ratios derived from satellite observations of the 2015 Indonesian fire plumes, Atmos. Chem. Phys., 16, 10111–10131, https://doi.org/10.5194/acp-16-10111-2016, 2016.

Pochanart, P., Akimoto, H., Kajii, Y., and Sukasem, P.: Carbon monoxide, regional-scale, and biomass burning in tropical continental Southeast Asia: Observations in rural Thailand, J. Geophys. Res.-Atmos., 108, 4552, https://doi.org/10.1029/2002JD003360, 2003.

Ravindra Babu, S., VenkataRatnam, M., Basha, G., Liou, Y.-A., and Narendra Reddy, N.: Large Anomalies in the Tropical Upper Troposphere Lower Stratosphere (UTLS) Trace Gases Observed during the Extreme 2015–16 El Niño Event by Using Satellite Measurements, Remote Sensing, 11, 687, https://doi.org/10.3390/rs11060687, 2019.

Ravindra Babu, S., Nguyen, L. S. P., Sheu, G.-R., Griffith, S. M., Pani, S. K., Huang, H.-Y., and Lin, N.-H.: Long-range transport of La Soufrière volcanic plume to the western North Pacific: Influence on atmospheric mercury and aerosol properties, Atmos. Environ., 268, 118806, https://doi.org/10.1016/j.atmosenv.2021.118806, 2022.

691 Ravindra Babu, S., Pani, S.K., Ou-Yang, C.F., Lin, N.H.: Impact of 21 June 2020 Annular Solar
692 Eclipse on Meteorological Parameters, O3 and CO at a High Mountain Site in Taiwan. Aerosol
693 Air Qual. Res. 22, 220248. https://doi.org/10.4209/aaqr.220248, 2022.

694 Reid, J. S., Hyer, E. J., Johnson, R., Holben, B. N., Yokelson, R. J., Zhang, J., Campbell, J. R.,
695 Christopher, S. A., Di Girolamo , L., Giglio, L., Holz, R. E., Kearney, C., Miettinen, J., Reid,
696 E. A.,Turk, F. J., Wang, J., Xian, P., Zhao, G., Balasubramanian, R., Chew, B. N., Janai, S.,
697 Lagrosas, N., Lestari, P., Lin, N.-H., Mahmud, M., Nguyen, A. X., Norris, B., Oahn, N. T. K.,
698 Oo, M., Salinas, S. V., Welton, E. J., Liew, S. C.: Observing and understanding the Southeast
699 Asian aerosol system by remote sensing: An initial review and analysis for the Seven Southeast
700 Asian Studies (7SEAS) program, Atmos. Res., 122, 403-468,
701 https://doi.org/10.1016/j.atmosres.2012.06.005, 2013.

702 Sheu, G.-R., Lin, N.-H., Wang, J-L., Lee,C-T.; Lulin Atmospheric Background Station: A New
703 High-Elevation Baseline Station in Taiwan, J-STAGE, Volume 24, Issue 2, Pages 84-89,
704 https://doi.org/10.11203/jar.24.84, 2009.

705 Tsay, S. C., Maring, H. B., Lin, N. H., Buntoung, S., Chantara, S., Chuang, H. C., Gabriel, P. M.,
706 Goodloe, C. S., Holben, B. N., Hsiao, T. C., Christina Hsu, N., Janjai, S., Lau, W. K. M., Lee,
707 C. Te, Lee, J., Loftus, A. M., Nguyen, A. X., Nguyen, C. M., Pani, S. K., Pantina, P., Sayer, A.
708 M., Tao, W. K., Wang, S. H., Welton, E. J., Wiriya, W. and Yen, M. C.: Satellitesurface
709 perspectives of air quality and aerosol-cloud effects on the environment: An overview of 7-
710 SEAS/BASELInE, Aerosol Air Qual. Res., 16(11), 2581–2602,
711 https://doi.org/10.4209/aaqr.2016.08.0350 , 2016.

712 van der Werf, G. R., Dempewolf, J., Trigg, S. N., Randerson, J. T., Kasibhatla, P. S., Giglio, L.,
713 Murdiyarso, D., Peters, W., Morton, D. C., Collatz, G. J., Dolman, A. J., and DeFries, R. S.:
714 Climate regulation of fire emissions and deforestation in equatorial Asia, Proc. Natl. Acad. Sci.
715 USA, 105, 20350–20355, https://doi.org/10.1073/pnas.0803375105, 2008.

716 van der Werf, G. R., Randerson, J. T., Giglio, L., van Leeuwen, T. T., Chen, Y., Rogers, B. M.,
717 Mu, M., van Marle, M. J. E., Morton, D. C., Collatz, G. J., Yokelson, R. J., and Kasibhatla, P.
718 S.: Global fire emissions estimates during 1997–2016, Earth Syst. Sci. Data, 9, 697–720,
719 https://doi.org/10.5194/essd-9-697-2017, 2017.

Wang, C.: ENSO, Atlantic climate variability, and the Walker and Hadley circulations, in: The Hadley circulation: Present, past and future, Springer, Berlin, 173–202, https://doi.org/10.1007/978-1-4020-2944-8_7, 2004.

Wang, S.-H., Welton, E. J., Holben, B. N., Tsay, S.-C., Lin, N.-H., Giles, D., Stewart, S. A., Janjai, S., Nguyen, X. A., Hsiao, T.-C., Chen, W.-N., Lin, T.-H., Buntoung, S., Chantara, S., and Wiriya, W.: Vertical Distribution and Columnar Optical Properties of Springtime Biomass-Burning Aerosols over Northern Indochina during 2014 7-SEAS Campaign, Aerosol Air Qual. Res., 15, 2037–2050, https://doi.org/10.4209/aaqr.2015.05.0310, 2015.

Weng, H. Y., Behera, S. K., and Yamagata, T.: Anomalous winter climate conditions in the Pacific rim during recent El Niño Modoki and El Niño events, Clim. Dynam., 32, 663–674, https://doi.org/10.1007/s00382-008-0394-6, 2009.

Whitburn, S., Van Damme, M., Clarisse, L., Turquety, S., Clerbaux, C., and Coheur, P.-F.: Doubling of annual ammonia emissions from the peat fires in Indonesia during the 2015 El Niño, Geophys. Res. Lett., 43, 11007–11014, https://doi.org/10.1002/2016gl070620, 2016.

Worden, J., Jiang, Z., Jones, D. B. A., Alvarado, M., Bowman, K., Frankenberg, C., Kort, E. A., Kulawik, S. S., Lee, M., Liu, J., Payne, V., Wecht, K., and Worden, H.: El Niño, the 2006 Indonesian peat fires, and the distribution of atmospheric methane, Geophys. Res. Lett., 40, 4938–4943, https://doi.org/10.1002/grl.50937, 2013.

Yin, Y., Ciais, P., Chevallier, F., van der Werf, G. R., Fanin, T., Broquet, G., Boesch, H., Cozic, A., Hauglustaine, D., Szopa, S., and Wang, Y.: Variability of fire carbon emissions in equatorial Asia and its nonlinear sensitivity to El Niño, Geophys. Res. Lett., 43, 10472–10479, https://doi.org/10.1002/2016gl070971, 2016.

744 **Table 1**. Detailed statistics of observed CO in October during 2006 to 2021 at LABS.

Year	Mean	Median	Standard Deviation	Change in CO (%)	Total data points
2006	**175.8**	**174**	**51**	**33.9**	**703**
2007	155.3	140	63.4	18.3	732
2008	125.5	125	26.9	-4.4	599
2009	127.1	125	35.5	-3.2	533
2010	143.9	136	38.1	9.6	739
2011	137.1	137	41.9	4.4	734
2012	155.8	153	39.4	18.7	643
2013	146.8	141	35.7	11.8	365
2014	125.6	120	39.8	-4.2	602
2015	**164.8**	**163.5**	**46.2**	**25.6**	**732**
2016	91.6	87	20.9	-30.2	732
2017	109.7	100.3	32.4	-16.4	744
2018	147.7	149.9	29.1	12.5	736
2019	142.4	142.8	37.7	8.5	742
2020	121.3	113.8	29.5	-7.5	742
2021	107.7	104.6	26.9	-17.9	744

745